

Grazing angle x-ray photoemission system for depth-dependent analysis

Terrence Jach and M. J. Chester

National Institute of Standards and Technology, Gaithersburg, Maryland 20899

S. M. Thurgate

School of Mathematical and Physical Sciences, Murdoch University, Murdoch 6150, W. A., Australia

(Received 7 September 1993; accepted for publication 22 October 1993)

We have developed an x-ray photoelectron spectrometer system which combines an adjustable grazing incidence angle source with reflected beam detection. When operated about the critical angle, this combination permits a variation of the x-ray penetration depth which can be monitored by means of the reflectivity. At angles of incidence less than the critical angle, the sampling depth of the photoemission is diminished, but the photoemission from the surface is enhanced due to the constructive interference of the incident and reflected x-ray beams. When used with Mg $K\alpha$ radiation ($E_\gamma=1253.6$ eV), the spectrometry system obtains useful distributions of chemical species in surface layers of 10–40 Å thickness. We present data showing the depth dependence obtained with the spectrometer of different oxides in a sulfide-treated, oxidized GaAs (100) surface.

I. INTRODUCTION

Various schemes have been employed to vary the depth of sampling in soft x-ray photoemission. The possibilities include changing the energy of the incident radiation,¹ changing the angle of takeoff of the photoelectrons,² and changing the angle of incidence of the radiation.³ In the last method, collimated x rays are incident at a grazing angle on an optically flat sample. At an angle of incidence less than or equal to the critical angle for total external reflection, the x-ray field within the sample is evanescent. The penetration depth of the x rays decreases as the angle of incidence is decreased towards zero.

Previously the angle of incidence has been varied by rotating the sample with respect to a fixed x-ray source and electron spectrometer.^{3,4} Changes in orientation of the sample with respect to either angle or distance from the electron spectrometer can lead to distortions in the energy distribution of escaping photoelectrons from the sample.⁵ These distortions can be comparable to the chemical shifts that might be observed in the x-ray photoemission line as the chemical environment changes with depth.

We describe here a system for performing grazing incidence x-ray photoemission spectroscopy (GIXPS) that eliminates the potential problems of rotating the sample, monitors the sample reflectivity, and calibrates the angle of incidence. The system incorporates a movable x-ray source in an ultrahigh vacuum (UHV) chamber and a fixed sample-electron spectrometer geometry. We demonstrate an example of its use in the investigation of oxide formation on a GaAs (100) surface which has been treated with a potentially passivating sulfide solution and then oxidized.

II. THEORY

There are several advantages to studying surface layers with x-ray photoemission, first considered by Henke.³ For atoms at a depth z beneath the surface, the contribution to the photoemission process is limited by both the extinction length λ_e of x rays incident at the surface and the attenu-

ation length λ_a of photoelectrons escaping to the surface. The sampling depth d may then be defined by

$$\frac{1}{d} = \frac{\cos \theta}{\lambda_e} + \frac{1}{\lambda_a},$$

where θ is the takeoff angle of the photoelectrons.

The index of refraction for soft x rays in matter takes the form

$$n = 1 - \delta - i\beta,$$

where δ and β are small. For x rays incident on a sample (Fig. 1) with an angle φ and a wave vector k , the solution inside the sample can be decomposed into components K_{\parallel} and K_{\perp} . It is readily shown that for small φ ,

$$K_{\perp} \approx k(\varphi^2 - 2\delta - 2i\beta)^{1/2}.$$

Since $\lambda_a = 4\pi/\text{Im}K_{\perp}$, going to angles $\varphi < (2\delta)^{1/2} \equiv \varphi_c$ provides a limitation on the sampling depth which is independent of the inelastic mean-free path of the photoelectrons. The limitation of λ_a also diminishes background due to inelastic scattering, as has been pointed out by Kawai *et al.*⁶

Furthermore, for $\varphi < \varphi_c$ the reflectivity of the surface increases. Since the reflected beam k' adds coherently with the incident beam k , there is an enhanced electric field at the surface and within the extinction depth of the surface for $\varphi < \varphi_c$. The Poynting vector of the solution within the surface is nearly parallel to the surface, making the transport of the radiation optimal for exciting atoms in the near surface region. The polarization vectors of the radiation at grazing incidence are also favorable for the emission of the photoelectrons in the direction of the detector.

Finally, in the case of an overlayer with a critical angle $\varphi_{c2} < \varphi_c$, it is possible to have x rays penetrating the overlayer and totally reflected from the overlayer-substrate interface. This results in a further enhancement of photoemission from the overlayer and diminished photoemission from the substrate.

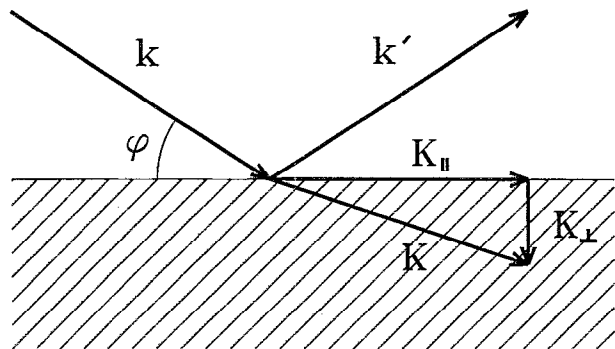


FIG. 1. Geometry of grazing incidence x-ray photoelectron spectroscopy system.

While it is desirable to obtain a large maximum and small minimum sampling depth, the choice of x-ray source energy is also influenced by the binding energy of the chemical species, the mean-free path of the photoelectrons, the energy range and resolution of the electron spectrometer, and the energy width of the x-ray source. For most materials and core levels, a GIXPS source energy in the range of 1–2 keV is most likely to be optimal.

Figure 2 shows the calculated sampling depth d in GaAs for Ga and As atom $3d$ levels excited by Mg $K\alpha$ x rays over a range of incidence angles. Curves are shown for two common electron spectrometers whose axes are normal to the sample surface: a hemispherical analyzer, which accepts electrons escaping the surface at normal takeoff angle, and a cylindrical mirror analyzer, which accepts electrons at 42° from normal. Although the change in sampling depth has a visible effect over layers thinner than the depths shown in the figure, the effect is maximized for layers comparable to the depth ranges shown. Consequently, layers with thicknesses between 10 and 40 Å, such

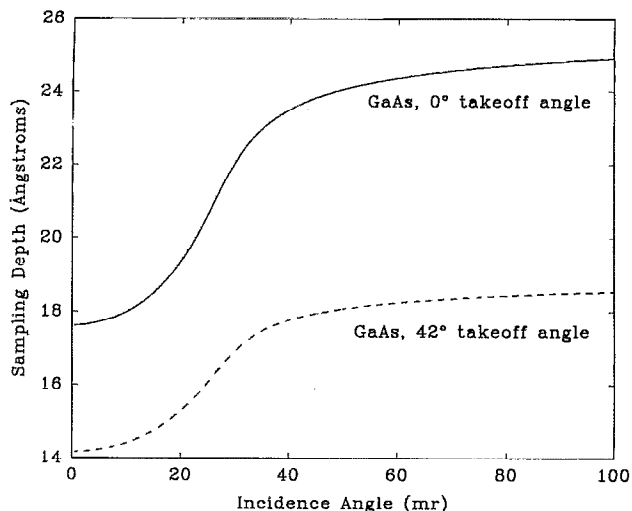


FIG. 2. Sampling depth of Mg $K\alpha$ x-ray photoemission as a function of incidence angle of the x rays on GaAs. Curves are shown for electron takeoff angles (from surface normal) of 0° and 42° .

as oxides on semiconductors, are most readily studied by means of this method. The critical angle φ_c for total external reflection from a variety of compounds in this energy range is typically 1.5° – 3° .

III. THE EXPERIMENTAL APPARATUS

The system as implemented in an UHV chamber is shown in Fig. 3. It consists of a collimated x-ray source, a sample mounted on a manipulator, an imaging x-ray detector, and an electron spectrometer. The source uses a Mg target (Mg $K\alpha$, $E_\gamma = 1253.6$ eV) and provides a collimated beam by a system of slits or parallel plates. During mea-

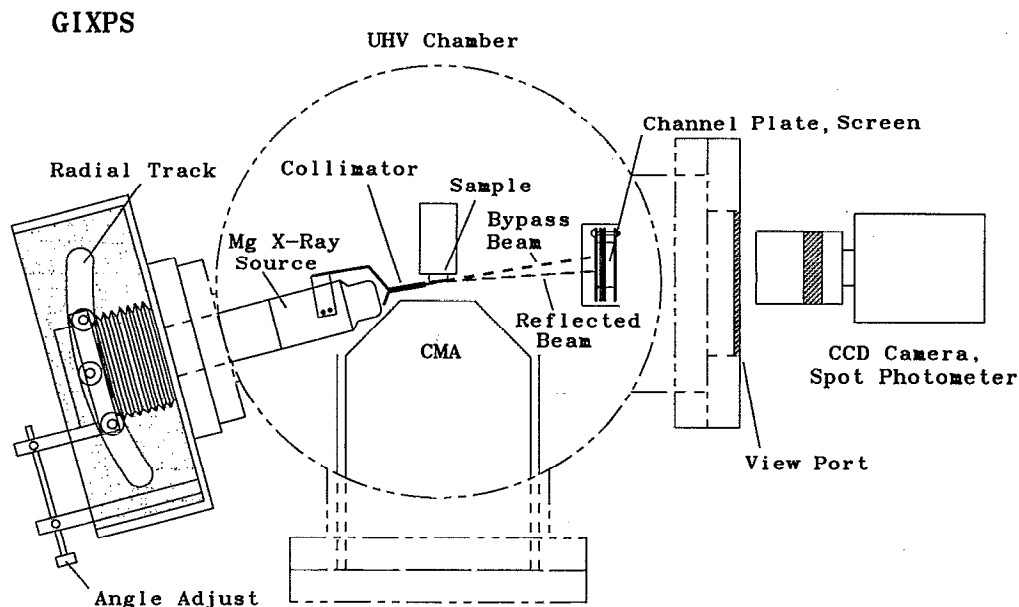


FIG. 3. GIXPS system implemented in an ultrahigh vacuum chamber. The electron spectrometer is a cylindrical mirror analyzer.

measurements that included both reflectivity and photoemission, the parallel plate collimator was used with a divergence of 0.7° . For measurements that did not include reflectivity, the collimator was replaced by a single slit. In either case, the combination of the slit and the area on the sample viewed by the electron spectrometer limited the beam divergence to 0.5° .

The x-ray source, mounted in a bellows, was constrained to move along a circular track outside the vacuum chamber. The track radius was chosen such that its origin coincided with the sample surface at the focus of the electron spectrometer, a double-pass cylindrical mirror analyzer. The collimator was aligned so that the spot illuminated on the target did not deviate by more than a few hundredths of a millimeter as the angle of incidence on the target was varied over 0° – 9° . The angle of incidence was set by means of a micrometer screw which could be adjusted either manually or by means of a stepping motor.

The sample was mounted on an UHV manipulator with heating capability. Because of the relatively large critical angles at the source energy, a standard UHV manipulator with a precision of 0.1° is sufficient to orient the sample.

The sample must be flat and optically polished so that it has a high x-ray reflectivity at the critical angle. This is monitored by means of an imaging detector capable of displaying both the straight-through beam from the collimated x-ray source and the portion of the beam reflected from the surface. The imaging detector was used to position the sample in the x-ray beam, measure reflectivity, and assure that the beam did not walk across the sample as the angle of incidence was varied.

The x-ray detector consists of a single-stage channel plate and a fluorescent screen. The reflected beam intensity is determined as a function of angle by means of either a spot photometer or a CCD camera and frame grabber. Figure 4 shows the reflected beam from a sample of GaAs wafer with only a commercial surface polish.

IV. RESULTS

Some results are presented here to demonstrate the operation of the system. The sample consisted of a GaAs(100) surface whose native oxide was etched away by means of a $\text{P}_2\text{S}_5/(\text{NH}_4)_2\text{S}$ solution which leaves S on the surface.⁷ The surface was then reoxidized by exposure to an UV/ozone treatment for 1 h. We observed the composition of the oxide which grew back in the presence of the surface sulfur. Previous studies had indicated that the depth of the oxide film was about 25 \AA thick.⁷

Figure 5 shows the x-ray reflectivity of the sample as determined by the channel plate using a spot photometer. The measurement was made with the Mg $K\alpha$ x-ray source operating at a power of 300 W. Figure 6(a) shows an As $3d$ GIXPS spectrum observed at an angle of incidence $\varphi=63 \text{ mrad}$ ($\varphi_c=27 \text{ mrad}$ for GaAs). X-ray photoelectron spectroscopy (XPS) count rates on the peaks of the lines were typically 3 c/s, resulting in a spectrum with reasonable statistics at a single angle for a counting time of 10 m/point.

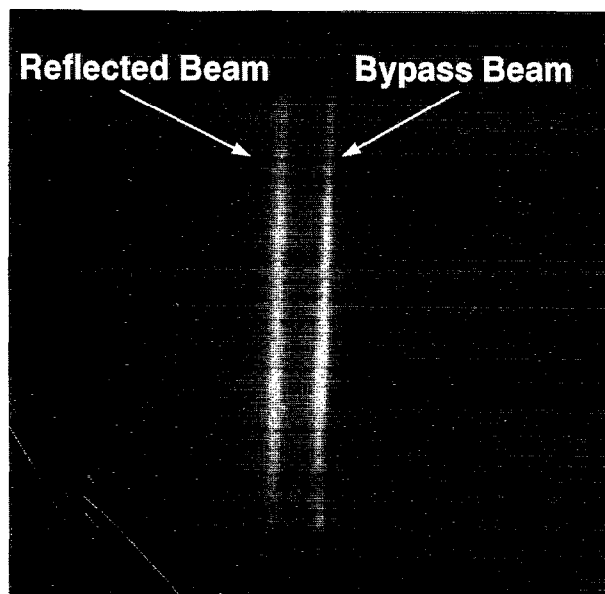


FIG. 4. Channel plate image of bypass x-ray beam and beam reflected from a GaAs wafer with a standard commercial polish.

Fits to Gaussian–Lorentzian peak shapes were used to extract the energies and peak areas of individual components. The width of each component, convolving the resolution of the unmonochromated Mg $K\alpha$ x-ray source, the instrument function of the double-pass CMA, and the width and splitting of the As $3d$ peaks was determined to be 1.8 eV. The resulting energies are indicative of As present in the As^{3+} and As^{5+} oxidation states as well as As in the native GaAs state.

Figure 6(b) shows the GIXPS spectrum for the more grazing incidence angle $\varphi=18 \text{ mrad}$. The As^{3+} and As^{5+} components are enhanced compared to the As line from

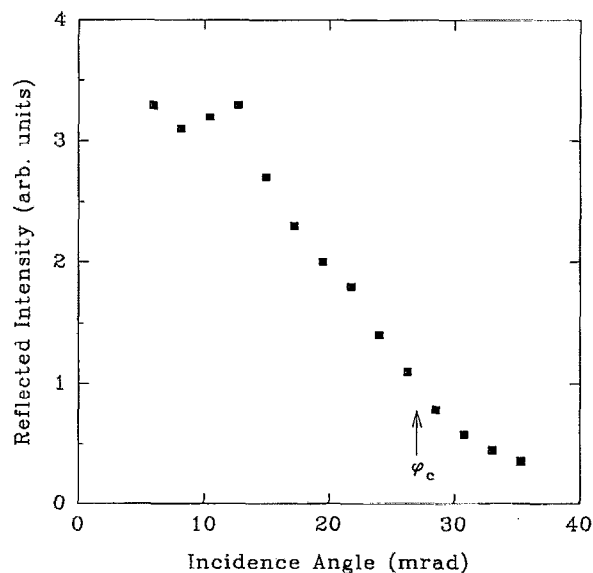


FIG. 5. X-ray reflectivity from a piece of GaAs wafer as a function of incidence angle. The reflectivity was measured by means of fluorescence intensity with a spot photometer. The critical angle is shown by an arrow.

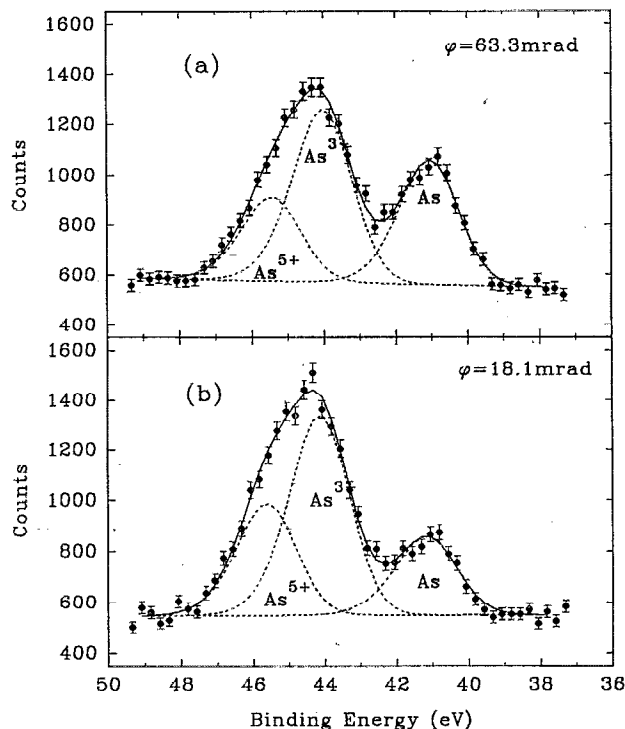


FIG. 6. (a) As 3d GIXPS spectrum for $\varphi=68$ mrad; (b) As 3d GIXPS spectrum for $\varphi=18$ mrad.

the underlying bulk GaAs. Data were collected over a range of incidence angles ($18 < \varphi < 63$ mrad). It should be noted that the critical angles for the oxides of GaAs differ very little from φ_c for bulk GaAs.

Figure 7 shows the peak areas for the different chemical species as a function of angle of incidence. The As peak decreases as the angle of incidence becomes smaller. The

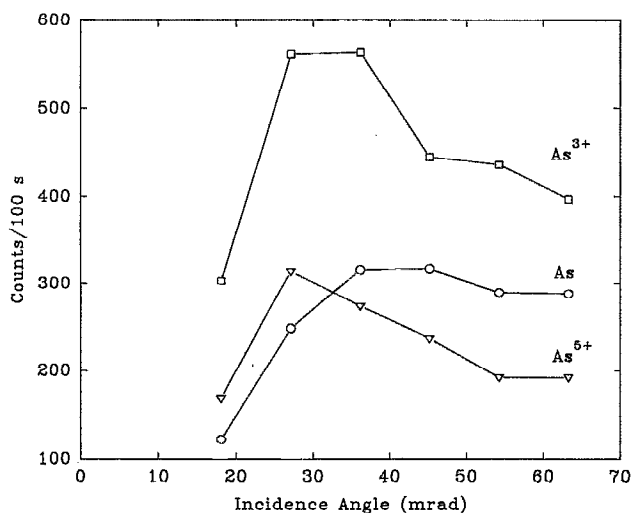


FIG. 7. Bulk As, As^{3+} , and As^{5+} components observed as a function of the angle of incidence.

As^{3+} and As^{5+} peaks increase until $\varphi \approx \varphi_c$ and then decrease in amplitude. This is indicative of chemical states which are located in a thin layer at the surface and which see an enhanced field due to reflection of the incident beam. The maximum enhancement of the As^{5+} states occurs at an angle smaller than the maximum enhancement of the As^{3+} states, indicating that the As closer to the surface is more highly oxidized than the As closer to the interface with the bulk GaAs. Quantitative depth information about the oxidation process can be extracted from the GIXPS data.^{8,9}

V. DISCUSSION

We have described an instrument for carrying out grazing incidence x-ray photoelectron spectroscopy to obtain the relative depths of chemical constituents present in thin layers on a surface. Since the method depends on the reflection of x rays from the optically flat surface of a sample, the system measures that reflectivity. The change in incidence angle is realized by the motion of the x-ray source which is always centered on the sample. The system maintains a fixed geometry between the sample and the electron spectrometer since changes in their relative positions might result in distortions in the photoemission line shapes.

When used with soft x rays the system is useful for obtaining information from surfaces where the distribution of constituents may vary over the top 10–40 Å. This depth range is particularly suitable for the study of the chemistry of oxides on semiconductors and metals.

We demonstrate the operation of the system with GIXPS spectra obtained from an oxide layer on a GaAs(100) surface, treated with a $\text{P}_2\text{S}_5/(\text{NH}_4)_2\text{S}$ solution and reoxidized afterwards. We observe the distribution of As^{5+} compounds closer to the surface and As^{3+} compounds closer to the interface with the native As of the substrate.

ACKNOWLEDGMENTS

We thank Dr. John Dagata for preparing the GaAs surfaces. The National Institute of Standards and Technology is part of the Technology Administration of the U.S. Department of Commerce.

- ¹W. Eberhardt, G. Kalkoffen, and C. Kunz, *Solid State Commun.* **32**, 901 (1979).
- ²P. H. Citrin, G. K. Wertheim, and Y. Baer, *Phys. Rev. B* **27**, 3160 (1983).
- ³B. L. Henke, *Phys. Rev. A* **6**, 94 (1972).
- ⁴M. Mehta and C. S. Fadley, *Phys. Lett. A* **55**, 59 (1975).
- ⁵N. E. Erickson and C. J. Powell, *Surface and Interface Anal.* **9**, 111 (1986).
- ⁶J. Kawai, M. Takami, M. Fujinami, Y. Hashiguchi, S. Hayakawa, and Y. Gohshi, *Spectrochim Acta Part B* **47**, 983 (1992).
- ⁷M. Chester, T. Jach, and J. A. Dagata, *J. Vac. Sci. Technol. A* **11**, 474 (1993).
- ⁸M. Chester, T. Jach, and S. M. Thurgate, *J. Vac. Sci. Technol. B* **11**, 1609 (1993).
- ⁹M. Chester and T. Jach, *Phys. Rev. B* **48**, 17262 (1993).